Optimal Control of Variable-Shape Wave Energy Converters*

Mohamed A. Shabara[1] and Ossama Abdelkhalik[2]

***Abstract*— This letter solves the optimal control problem for variable-shape wave energy converters analytically, where Pontryagin's minimum principle is applied to get the control laws. The optimal control solution for the conventional fixed-shape wave energy converters requires power take-off units with bidirectional power flow capability; this means that it can harvest energy from the waves at certain times and act as an actuator at other instants to keep the system in resonance with the ocean waves. This bidirectional capability requires designing complex and expensive power take-off units. The variable shape wave energy converters were recently introduced to reduce the need for this bidirectional power capability. The main contribution of this letter is to derive the optimal control laws for variable-shape wave energy converters for the flexible passive shell and flexible controlled shell. The optimal control that maximizes the harvested energy is found to include both bang-bang and singular arc phases.**

I. INTRODUCTION

WAVE energy is sustainable and is an abundant renewable energy source characterized by its high power density [1]. However, wave power has the disadvantage of being highly idiosyncratic, and with a high Levelized cost of energy (LCoE). A Wave Energy Converter (WEC) system is divided into four subsystems [2]: (1) hydrodynamic subsystem, (2) power take-off (PTO) subsystem, (3) reaction subsystem, and (4) control and instrumentation subsystem. The hydrodynamic subsystem captures/harvests the wave energy, e.g., point absorbers [3], [4], overtopping devices, and oscillating water columns. The PTO converts the harvested wave energy into electrical energy (e.g., hydraulic PTO, and linear generators). The reaction subsystem anchors the WEC into a specific location or reference point (e.g., mooring systems). The control subsystem controls the movement of the WEC to maximize the power generation mostly to create a mechanical impedance matching in the WEC system.

The equation of motion for a single degree of freedom (DoF) fixed shape buoy (FSB) WEC was derived by W.E. Cummins in the context of modeling of ship motion [5]:

$$m\ddot{x}(t) = \overbrace{\int_{-\infty}^{\infty} h_{\text{ext}}(\tau)\eta(t-\tau,x)d\tau}^{\text{Excitation force } f_{\text{ext}}} + f_{\text{h}}(t) \underbrace{-m_{\infty}\ddot{x}(t) - \int_{-\infty}^{t} h_{\text{rad}}(\tau)\dot{x}(t-\tau)d\tau}_{\text{Radiation force } f_{\text{rad}}} - u(t) \quad (1)$$

where m, and m_{∞} are the mass of the buoy and the hydrodynamic added mass, respectively, x is a map, $x(t), \dot{x}(t)$, and $\ddot{x}(t) \in \mathbb{R}$ are the heave displacement, velocity, and acceleration, respectively; $\mathbb{R}$ is the set of real numbers. $\eta \in \mathbb{R}$ is the wave elevation, $f_{\text{h}} \in \mathbb{R}$ is the hydrostatic force, f_{ext} and $f_{\text{rad}} \in \mathbb{R}$ are the excitation and radiation forces due to the impulse functions h_{ext} and h_{rad}, respectively. The control force $u(t)$ is the force that is exerted on the buoy by the PTO. On the other hand, the equation of motion for a single DoF (heave) variable-shape buoy wave energy converter (VSB WEC) can be expressed as [6]:

$$\boldsymbol{M}\ddot{\mathbf{x}}(t)+\boldsymbol{D}\dot{\mathbf{x}}(t)+\boldsymbol{K}\mathbf{x}(t) = \overbrace{\int_{-\infty}^{\infty} \boldsymbol{h}_{\text{ext}}(\tau)\eta(t-\tau,\mathbf{x})d\tau}^{\text{Generalized excitation force } \boldsymbol{Q}_{\text{ext}}} + \boldsymbol{Q}_{\text{h}}(t) \underbrace{-\boldsymbol{M}_{\infty}(t)\ddot{\mathbf{x}}(t) - \int_{-\infty}^{t} \boldsymbol{h}_{\text{rad}}(\tau)\dot{\mathbf{x}}(t-\tau)d\tau}_{\text{Generalized radiation force } \boldsymbol{Q}_{\text{rad}}} - \boldsymbol{Q}_{\text{pto}}(t) + \boldsymbol{Q}_{\text{c}}(t) \quad (2)$$

where the generalized coordinates are used in the equation above, $\mathbf{x}$ is a map, $\mathbf{x}(t) \in \mathbb{R}^{N_p \times 1}$ is the generalized state vector such that $N_p = N + \text{DoF}$, and $N \in \mathbb{Z}_+$ is the number truncated terms of the mode shapes of the flexible buoy and DoF for heave only motion is 1. $\boldsymbol{M}$ and $\boldsymbol{M}_{\infty}(t) \in \mathbb{R}^{N_p \times N_p}$ are the generalized mass and the generalized added mass coefficient matrices, respectively. The generalized added mass is a function of time since the shape of the buoy changes actively with the incident waves. The $\boldsymbol{D}$ and $\boldsymbol{K} \in \mathbb{R}^{N_p \times N_p}$ are the generalized damping and stiffness matrices related to the buoy's shell material. The generalized forces $\boldsymbol{Q}_{\text{ext}}(t)$ and $\boldsymbol{Q}_{\text{rad}}(t) \in \mathbb{R}^{N_p \times 1}$ are computed based on the impulse functions $\boldsymbol{h}_{\text{ext}}$ and $\boldsymbol{h}_{\text{rad}}$, respectively; finally $\boldsymbol{Q}_{\text{c}}(t) = \boldsymbol{A}^T\boldsymbol{\lambda}$, $\boldsymbol{Q}_{\text{h}}(t)$, $\boldsymbol{Q}_{\text{pto}}(t) \in \mathbb{R}^{N_p \times 1}$ are the generalized constraint, hydrostatic and control forces, where $\boldsymbol{\lambda} \in \mathbb{R}^{3\times 1}$ is the column matrix of Lagrange multipliers and $\boldsymbol{A} \in \mathbb{R}^{3\times N_p}$ is the Jacobian constraint matrix [7]. The optimal control solution for fixed-shape WECs has been addressed in many references; however, the optimal control of ***variable-shape*** WECs was not addressed before, which is the main contribution of this letter.

*This work was supported by the National Science Foundation (NSF)

[1]Mohamed Shabara is a Ph.D. student in the Aerospace Engineering Department, Iowa State University, Ames, IA 50011, USA mshabara@iastate.edu

[2]Ossama Abdelkhalik is a Professor in the Aerospace Engineering Department, Iowa State University, Ames, IA 50011, USA ossama@iastate.edu

A. Notation

The set of real and complex numbers are denoted by $\mathbb{R}$ and $\mathbb{C}$, respectively. $|\cdot|$ is the Euclidean norm, and, the set of positive integers is represented as $\mathbb{Z}_+$. Identity matrix $\boldsymbol{I}_{N\times N} = \begin{bmatrix}\mathbf{1}_1 & \mathbf{1}_2 & \dots & \mathbf{1}_N\end{bmatrix}$, $\Re$ and $\Im$ are the real and imaginary parts, $i = \sqrt{-1}$, and $\bar{A}$ denoted the averaged A.

B. Related Work

The problem of optimal control of a VSB WEC has received minimal attention; therefore, this section highlights the optimal control strategies in the literature for FSB WECs, before the optimal control of VSB WECs is developed in the following sections. Most of the PTO optimal control formulations are in the category of phase and amplitude control, or impedance matching (IM) control (reactive control). The IM principle states a general condition for optimal energy capture under standard linear assumptions. Some reactive controllers approximate the IM condition at one single frequency [8], while alternative controllers, like the LiTe-Con [9], provide a broadband approximation of the IM condition.

The optimal resistive loading (ORL) control ($u(t) = -c^*\dot{x}(t)$) [10] and the latching and unlatching [11] control methods are passive control strategies that are easy to implement. For the latching control, the WEC is unlatched when it is in phase with the waves, and it is latched when it is out of phase. The "*" denotes the optimum value, and $c \in \mathbb{R}_+$ is the damping coefficient.

Ref. [12] used genetic algorithms to parameterize the damping profile based on a sigmoid function; genetic algorithms were also used in conjunction with neural network to achieve the same control objective [12]. Fuzzy logic was also implemented to control WECs such that the controller adjust the damping and stiffness of the PTO to create mechanical IM [13]. References [14], and [15] used reinforcement learning, with a time-varying proportional derivative (PD) control law, to realize mechanical IM in the system such that $u^*(t) = -K_p(t)x(t) - K_d(t)\dot{x}(t)$, where the control gains were defined by the deep Q-Network (DQN). Ref. [10] used Pontryagin's minimum principle (PMP) to obtain the optimal control law for FSB WECs where it was found that the control law follows a band-singular-bang behavior and the singular arc law is expressed as: $u^{\text{sa}}(t) = f_{\text{ext}}(t) - kx(t) - c\dot{x}(t) - \frac{m}{2c}\frac{\partial f_{\text{ext}}}{\partial t}$; the coefficient $k \in \mathbb{R}_+$ is the hydrostatic stiffness coefficient.

Reference [16] used the PMP to derive the optimal control for point absorbers (PA) with a PTO that incorporated both linear damping and active control elements; the optimal control was shown in [16] to be bang-bang when constraints are imposed only on the PTO force. Although the PMP analysis was done on a single DoF PA, this method can be generalized to account for multiple degrees of freedom. This letter follows a similar approach as Ref. [16]; however, the analysis is carried out for VSB WECs, and the resulting control law is a combination of bang-bang and singular arc controls.

In complex-conjugate control [17], the optimal reactance $X_{\text{pto}} = \Im\{Z_{\text{pto}}(\omega) = -U(\omega)/V(\omega)\}$ is chosen such that it cancels out the intrinsic mechanical reactance of the system, where Z_{pto} is the PTO impedance, $U(\omega)$, and $V(\omega)$ are the frequency domain PTO force and velocity, respectively. The reactance of the PTO is non-zero ($i.e., X_{\text{pto}} \neq 0$), which results in a bidirectional effect in which the PTO harvests energy at some time intervals $t \subset T \subset \mathbb{R}_+$ and returns power to the water at time intervals $t \not\subset T \subset \mathbb{R}_+$. By definition, when the incident wave matches the natural frequency of the system, then $X_{\text{pto}} = 0$. To obtain the bidirectional power behavior, the PTO requires more expensive components causing an increase in the running and initial costs.

C. Contribution

VSB WECs were introduced to reduce or rather eliminate the need for reactive power [18], i.e., design WECs that are economically more convenient. The VSB WECs have a jellyfish like behavior, such that part of the spring-like behavior of the reactive control is removed from the PTO and placed in the buoy itself. Previous work in the literature aimed at understanding the physics and behavior of the VSB WEC using passive damping and bang-bang controls [6], [7], [19], but the optimal control problem was not attempted. This letter represents the first work to derive the optimal control law for VSB WECs to maximize power extraction. PMP is used to obtain the control laws; it was found that the VSB requires less reactive power to harvest a larger amount of energy; the derived optimal control law is a combination of singular arc and bang-bang control laws.

II. DYNAMIC MODEL AND PROBLEM STATEMENT

This section discusses the dynamics and the equation of motion for VSB WECs, then the optimal control problem is formulated as a first step to derive the control laws.

A. System Model

References [6] and [7] used the first principals of analytical mechanics to derive the equation of motion for VSB WECs, the distributed parameter associated with the shell deformation vector ($\vec{\boldsymbol{r}}_{dmc} = [u \;\; w \;\; v] \in \mathbb{R}^3$) shown in Fig. 1 was converted to a discrete parameter using the Rayleigh-Ritz approximation, where the shell deformation vector, assuming no deformation perpendicular to the page, is expressed as [6]:

$$\vec{\boldsymbol{r}}_{dmc}(\phi, t) = [\boldsymbol{\Psi}_e^{\phi^T}(\phi) \;\; \mathbf{0}^T \;\; \boldsymbol{\Psi}_e^{r^T}(\phi)]^T \boldsymbol{\eta}(t) = \boldsymbol{\Phi}_e \boldsymbol{\eta}(t) \tag{3}$$

where the functions $\boldsymbol{\Psi}_e^{\phi}(\phi)$, $\boldsymbol{\Psi}_e^{r}(\phi) : \mathbb{R}^{1\times N}$ are trial (admissible) functions that follow the Legendre polynomial of the first kind [6], [7], these functions describe the mode shapes of the axisymmetric vibrations of spherical shells. The angle ϕ describes the location of an infinitesimal mass "dm" on the non-deformed shell; it is the angle between the third axis of the body reference frame $\boldsymbol{s}_3$ and the normal to the non-deformed shell $\boldsymbol{e}_3$ as shown in Fig. 1, and $\boldsymbol{\eta} \in \mathbb{R}^N$ is the time-dependent Rayleigh-Ritz coefficients vector. References

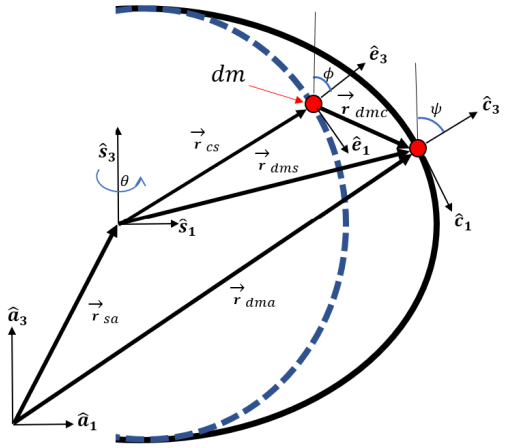

Fig. 1. Kinematic representation of the VSB, (solid black line: deformed buoy, and dashed black line: non-deformed Buoy [6], [7]

[6] and [7] have a full kinematic description for the VSB. Eq. (2) can be expressed as [6]:

$$\tilde{\boldsymbol{M}}(t)\ddot{\mathbf{x}}+\boldsymbol{D}\dot{\mathbf{x}}+\tilde{\boldsymbol{K}}(t)\mathbf{x}=\boldsymbol{A}^T\boldsymbol{\lambda}+\boldsymbol{Q}_{\text{ext}}(t)+\boldsymbol{Q}_{\text{rad}}(t,\dot{\mathbf{x}})+\boldsymbol{Q}_{\text{pto}}(t) \quad (4)$$

where $\mathbf{x} = [\vec{\boldsymbol{r}}_{sa,3} \quad \boldsymbol{\eta}^T]^T \in \mathbb{R}^{N_p\times 1}$, $\tilde{\boldsymbol{M}}(t) = \boldsymbol{M} + \boldsymbol{M}_\infty(t) \in \mathbb{R}^{N_p\times N_p}$ such that $\boldsymbol{M}_\infty(t) = \lim_{\omega\to+\infty}\boldsymbol{M}_\omega(t)$, and $\tilde{\boldsymbol{K}}(t) = \boldsymbol{K}+\boldsymbol{K}_{\text{h}}(t) \in \mathbb{R}^{N_p\times N_p}$, where $\boldsymbol{K}_{\text{h}}$ is the generalized hydrodynamic stiffness coefficient and its expression can be found in Ref. [6], and $\vec{\boldsymbol{r}}_{sa}$ is a vector that describes the center of gravity "C.G" position of the buoy with respect to the inertial reference frame $\hat{\boldsymbol{a}}$ (Fig.1).

Also, $\boldsymbol{M} = \text{diag}[m \quad \boldsymbol{M}_{ee}]$ such that $m \in \mathbb{R}_+$, and $\boldsymbol{M}_{ee} \in \mathbb{R}^{N\times N}$ are the mass, and the generalized mode shape mass matrices. Additionally, $\boldsymbol{D} = \text{diag}[c \quad \boldsymbol{D}_{ee}]$, and $\boldsymbol{K} = \text{diag}[k \quad \boldsymbol{K}_{ee}]$, where the damping c and stiffness k are scalar quantities related to the translational motion of C.G, $\boldsymbol{D}_{ee}$ and $\boldsymbol{K}_{ee} \in \mathbb{R}^{N\times N}$ are diagonal generalized damping and stiffness matrices related to the generalized mode shapes for the flexible buoy.

The external forces are (1) the generalized constraint force $\boldsymbol{Q}_{\text{c}} = \boldsymbol{A}^T\boldsymbol{\lambda}$ which accounts for the constraints applied to the buoy's shape and C.G motions; in this work, $\boldsymbol{Q}_{\text{c}} = \mathbf{0}$, (2) the generalized PTO force $\boldsymbol{Q}_{\text{pto}}(t)$, (3) the generalized excitation force $\boldsymbol{Q}_{\text{ext}}(t) = \sum_{j=1}^{N_\omega}\Re(\boldsymbol{E}_{\boldsymbol{x}j}(t,\omega_j)\eta_j e^{i(\omega_j t+\phi_j)})$ such that $N_w \in \mathbb{Z}_+$ is the number of waves, and $\boldsymbol{E}_{\boldsymbol{x}}(t,\omega) \in \mathbb{C}^{N_p\times N_\omega}$ is the generalized excitation force coefficient, η_j, $\omega_j \in \mathbb{R}_+$ are the j^{th} wave elevation and frequency, and (4) the generalized hydrodynamic radiation force "$\boldsymbol{Q}_{\text{rad}}(t)$". For irregular waves [6]:

$$\boldsymbol{Q}_{\text{rad}}(t,\mathbf{x}_2) = -\int_0^t (\boldsymbol{K}(t-\tau)\mathbf{x}_2(\tau))\,d\tau \quad (5)$$

where $\boldsymbol{K} \in \mathbb{R}^{N_p\times N_p}$ is the retardation function that describes the fluid memory effects, and it is expressed as $\boldsymbol{K}(t) = \frac{2}{\pi}\int_{\omega_{\min}}^{\omega_{\max}}\boldsymbol{D}_{\text{rad}}(t,\omega)\cos(\omega t)\,d\omega$. Also, $\boldsymbol{D}_{\text{rad}}(t,\omega) \in \mathbb{R}^{N_p\times N_p}$ is the generalized radiation damping coefficient, which is available in Ref. [6].

For regular waves, the generalized hydrodynamic radiation force can expressed as $\boldsymbol{Q}_{\text{rad}}(t) = \boldsymbol{D}_{\text{rad}}(t)\mathbf{x}_2(t)$.

Solving Eq. (4) requires solving a two-way fluid-structure interaction (FSI) model; the generalized hydrodynamic coefficients are calculated from the pressures obtained from the potential flow theory, and the BEM solvers, which are computationally expensive to solve at every time step. To solve that computational time problem, Ref [6] proposed treating the problem as a one-way FSI problem by averaging the time-dependent coefficients using the Reynolds decomposition method such that $\boldsymbol{M}_\infty(t), \boldsymbol{D}_{\text{rad}}(t), \boldsymbol{K}_{\text{h}}(t), \boldsymbol{E}_{\boldsymbol{x}}(t) \longrightarrow \bar{\boldsymbol{M}}_\infty, \bar{\boldsymbol{D}}_{\text{rad}}, \bar{\boldsymbol{K}}_{\text{h}}, \bar{\boldsymbol{E}}_{\boldsymbol{x}}$. Accordingly Eq. (4) becomes [6]:

$$\bar{\boldsymbol{M}}\ddot{\mathbf{x}} + \boldsymbol{D}\dot{\mathbf{x}} + \bar{\boldsymbol{K}}\mathbf{x} = \boldsymbol{A}^T\boldsymbol{\lambda} + \bar{\boldsymbol{Q}}_{\text{ext}}(t) + \boldsymbol{Q}_{\text{pto}}(t) + \bar{\boldsymbol{Q}}_{\text{rad}}(t) \quad (6)$$

where the overbar denotes the averaged value. Treating the problem as a one-way FSI problem was mainly needed to reduce the computational time required to solve the VSB WEC problems; however, it introduced an error of $\pm 2\%$ in the total harvested energy [6]; furthermore, even with accurately calculated averaged values, the resolution of the physics of the problem is reduced.

B. PROBLEM STATEMENT

PMP is applied in this work. This principle screens the potential solutions at each time step and can identify the candidate that minimizes the Hamiltonian if it exists and is unique. On the other hand, there are cases when there is an infinite number of candidates, or the stationary condition is not an explicit function of the control force, i.e., the stationary condition does not furnish any information about the control law. This condition is demonstrated in this letter.

The objective of the optimal control problem $\mathcal{J}$ is to maximize the harvested energy for time $t \in [0, t_f]$ such that $\mathcal{J} = -\int_0^{t_f}\boldsymbol{Q}_{\text{pto}}^T\mathbf{x}_2$, where $\boldsymbol{Q}_{\text{pto}}^T = [u_1 \quad \boldsymbol{u}_2^T]$ accounts for the PTO force on the C.G. ($u_1 \in \mathbb{R}^1$), and $\boldsymbol{u}_2 \in \mathbb{R}^{N\times 1}$ is the control force acting on the shell assuming the use of piezoelectric harvesters/actuators on the buoy's surface. The optimal control problem for regular waves can be treated as a particular case of the optimal control problem of irregular by replacing the expression for "$\bar{\boldsymbol{Q}}_{\text{rad}}(t)$"; therefore, in this letter, the optimal control problem for irregular waves will be solved, then a particular solution is presented for regular waves. The optimal control problem for irregular waves can be formulated based on Eq. (6) and expressed as

$$\begin{aligned}
\min_{\mathbf{x}_2, \boldsymbol{Q}_{pto}} \quad & \mathcal{J} = -\int_{t_0}^{t_f}\boldsymbol{Q}_{\text{pto}}^T\mathbf{x}_2 dt \\
\text{s.t.} \quad & \dot{\mathbf{x}}_1 = \mathbf{x}_2, t \in [t_0, t_f], \\
& \dot{\mathbf{x}}_2 = \bar{\boldsymbol{M}}^{-1}\left(-\boldsymbol{D}\mathbf{x}_2 - \bar{\boldsymbol{K}}\mathbf{x}_1 + \bar{\boldsymbol{Q}}_{\text{hydro}} - \boldsymbol{Q}_{\text{pto}}\right), \\
& \dot{x}_3 = 1, \mathbf{x}_{10} = \mathbf{x}_1(t_0), \mathbf{x}_{20} = \mathbf{x}_2(t_0)
\end{aligned}$$

where $\bar{\boldsymbol{Q}}_{\text{hydro}} = \bar{\boldsymbol{Q}}_{\text{ext}}(x_3) + \bar{\boldsymbol{Q}}_{\text{rad}}(\mathbf{x}_2, x_3) \in \mathbb{R}^{N_p\times 1}$. Note that this problem can be formulated in terms of the generalized radiation states $\mathbf{x}_r$, rather than the generalized radiation force that is calculated using the convolution. Noting that the system is non-autonomous, hence, time is considered as a state $x_3 \in \mathbb{R}$.

The control limits for the optimal control problem is:

$$\boldsymbol{Q}_{\text{pto}} \in U \triangleq \{\boldsymbol{Q}_{\text{pto}} : \boldsymbol{Q}_{\text{pto}}^{\min} \le \boldsymbol{Q}_{\text{pto}} \le \boldsymbol{Q}_{\text{pto}}^{\max}\} \forall t \in [t_0, t_f] \quad (7)$$

III. MATH: OPTIMAL CONTROL

In this section, the optimal control laws for VSB WECs in irregular waves and regular waves are derived. The derivation procedure is as follows: we first construct the Hamiltonian H, then we derive the necessary conditions for optimality, which include the adjoint equations $\dot{\boldsymbol{\lambda}} = -\partial H/\partial \mathbf{x}$, where $\boldsymbol{\lambda}$ is the vector of Lagrange multipliers, and the stationary condition $H_u = -\partial H/\partial \boldsymbol{Q}_{pto}^T$ [16].

In this letter, no mechanical damping force is applied on the C.G (i.e., $c = 0$), and the generalized damping matrix $\boldsymbol{D}$ in Eq. (6) becomes singular. The Hamiltonian of this problem can be constructed as

$$H\big(\mathbf{x}, \boldsymbol{\lambda}, \boldsymbol{Q}_{\text{pto}}\big) = -\boldsymbol{Q}_{\text{pto}}^T \mathbf{x}_2 + \boldsymbol{\lambda}_1^T \mathbf{x}_2 + \boldsymbol{\lambda}_2^T \bar{\boldsymbol{M}}^{-1} \times \big(-\boldsymbol{D}\mathbf{x}_2 - \bar{\boldsymbol{K}}\mathbf{x}_1 + \bar{\boldsymbol{Q}}_{\text{ext}} + \bar{\boldsymbol{Q}}_{\text{rad}} - \boldsymbol{Q}_{\text{pto}}\big) + \lambda_3 \quad (8)$$

The Hamiltonian is linear with respect to the PTO force $\boldsymbol{Q}_{\text{pto}}$, which means that the stationary condition is not an explicit function of the control force, and a singular arc solution will be obtained. The adjoint equations are expressed as:

$$\dot{\boldsymbol{\lambda}}_1 = \Big(\bar{\boldsymbol{M}}^{-1}\bar{\boldsymbol{K}}\Big)^T \boldsymbol{\lambda}_2 \quad (9)$$

$$\dot{\boldsymbol{\lambda}}_2 = \boldsymbol{Q}_{\text{pto}} - \boldsymbol{\lambda}_1 + \Big(\bar{\boldsymbol{M}}^{-1}\big(\boldsymbol{D} - \frac{\partial \bar{\boldsymbol{Q}}_{\text{rad}}^T}{\partial \mathbf{x}_2}\big)\Big)^T \boldsymbol{\lambda}_2 \quad (10)$$

$$\dot{\lambda}_3 = -\left(\bar{\boldsymbol{M}}^{-1}\Big(\frac{\partial}{\partial x_3}\Big(\bar{\boldsymbol{Q}}_{\text{ext}} + \bar{\boldsymbol{Q}}_{\text{rad}}\Big)\Big)^T \boldsymbol{\lambda}_2\right) \quad (11)$$

The stationary condition is then expressed as:

$$H_u = -\mathbf{x}_2 - \bar{\boldsymbol{M}}^{-T}\boldsymbol{\lambda}_2 = \mathbf{0} \Longleftrightarrow \boldsymbol{\lambda}_2 = -\bar{\boldsymbol{M}}^T \mathbf{x}_2 \quad (12)$$

The stationary condition does not yield an expression for the control force "$\boldsymbol{Q}_{\text{pto}}$", the high order maximum principle (HMP) may be used to obtain additional necessary conditions to derive the control law [16]. The additional necessary conditions are obtained by differentiating the Hamiltonian with respect to time $k \in \mathbb{Z}_+$ number of times until the following form is obtained $\frac{d^{2k}}{dt^{2k}} H_u\big(\mathbf{x}, \boldsymbol{Q}_{\text{pto}}, \boldsymbol{\lambda}\big) = \boldsymbol{G}_0 + \boldsymbol{G}_1 \boldsymbol{Q}_{\text{pto}}(t) = \mathbf{0}$, where k is the order of singularity and the control law becomes $\boldsymbol{Q}_{\text{pto}} = -\boldsymbol{G}_0/\boldsymbol{G}_1$, where $\boldsymbol{G}_1 \neq \mathbf{0}\ \ \forall t \in [t_1, t_2]$. The first additional necessary condition is obtained by differentiating Eq. (12) to get:

$$\dot{H}_u = -\dot{\mathbf{x}}_2 - \bar{\boldsymbol{M}}^{-T}\dot{\boldsymbol{\lambda}}_2 = \mathbf{0} \Longleftrightarrow \dot{\boldsymbol{\lambda}}_2 = -\bar{\boldsymbol{M}}^T \dot{\mathbf{x}}_2 \quad (13)$$

Substituting Eq. (9) into Eq. (12) then integrating yields:

$$\boldsymbol{\lambda}_1 = -\bar{\boldsymbol{K}}^T \mathbf{x}_1 - \boldsymbol{C} \quad (14)$$

where $\boldsymbol{C} \in \mathbb{R}^{N_p \times 1}$ is an integration constant. Substitute Eq. (14), the 2[nd] constraint, and Eq. (10) in Eq. (13) we get:

$$\dot{H}_u = \bar{\boldsymbol{C}}_3 \boldsymbol{Q}_{\text{pto}} + \bar{\boldsymbol{C}}_2 \mathbf{x}_2 + \bar{\boldsymbol{C}}_1 \mathbf{x}_1 - \bar{\boldsymbol{M}}^{-1}\big(\bar{\boldsymbol{Q}}_{\text{ext}} + \bar{\boldsymbol{Q}}_{\text{rad}}\big) - \Big(\bar{\boldsymbol{M}}^{-T}\frac{\partial \bar{\boldsymbol{Q}}_{\text{rad}}}{\partial \mathbf{x}_2}\Big)\mathbf{x}_2 - \boldsymbol{C} = \mathbf{0} \quad (15)$$

where $\bar{\boldsymbol{C}}_3 = \big(\bar{\boldsymbol{M}}^{-1} - \bar{\boldsymbol{M}}^{-T}\big)$, $\bar{\boldsymbol{C}}_2 = (\bar{\boldsymbol{M}}^{-1}\boldsymbol{D} + (\boldsymbol{D}\bar{\boldsymbol{M}}^{-1})^T)$, and $\bar{\boldsymbol{C}}_1 = (\bar{\boldsymbol{M}}^{-1}\bar{\boldsymbol{K}} + (\bar{\boldsymbol{K}}\bar{\boldsymbol{M}}^{-1})^T)$, the expression in $\bar{\boldsymbol{C}}_3$ is skew-symmetric, i.e., it is a coupling matrix for the generalized control force elements; $\partial \dot{H}_{u_1}/\partial u_1 = 0$ and $\partial \dot{H}_{\boldsymbol{u}_2}/\partial \boldsymbol{u}_2 = \mathbf{0}$.

Differentiating Eq. (15) to get an additional necessary condition yields:

$$\ddot{H}_u = \bar{\boldsymbol{C}}_3 \frac{\partial \boldsymbol{Q}_{\text{pto}}}{\partial x_3} + \Big(\bar{\boldsymbol{C}}_2 - \bar{\boldsymbol{M}}^{-T}\frac{\partial \bar{\boldsymbol{Q}}_{\text{rad}}}{\partial \mathbf{x}_2}\Big)\dot{\mathbf{x}}_2 + \bar{\boldsymbol{C}}_1 \mathbf{x}_2 - \bar{\boldsymbol{M}}^{-1}\frac{\partial}{\partial x_3}\Big(\bar{\boldsymbol{Q}}_{\text{ext}} + \bar{\boldsymbol{Q}}_{\text{rad}}\Big) - \Big(\bar{\boldsymbol{M}}^{-T}\frac{\partial \bar{\boldsymbol{Q}}_{\text{rad}}}{\partial x_3 \partial \mathbf{x}_2}\Big)\mathbf{x}_2 = \mathbf{0} \quad (16)$$

Rearranging Eq. (16) yields:

$$\dot{\mathbf{x}}_2 = \Big(\bar{\boldsymbol{C}}_2 - (\bar{\boldsymbol{M}}^{-T}\frac{\partial \bar{\boldsymbol{Q}}_{\text{rad}}}{\partial \mathbf{x}_2})\Big)^{-1}\Big[\bar{\boldsymbol{M}}^{-1}\frac{\partial}{\partial x_3}\Big(\bar{\boldsymbol{Q}}_{\text{ext}} + \bar{\boldsymbol{Q}}_{\text{rad}}\Big) - \bar{\boldsymbol{C}}_3 \frac{\partial \boldsymbol{Q}_{\text{pto}}}{\partial x_3} + \Big((\bar{\boldsymbol{M}}^{-T}\frac{\partial^2 \bar{\boldsymbol{Q}}_{\text{rad}}}{\partial \mathbf{x}_2 \partial x_3}) - \bar{\boldsymbol{C}}_1\Big)\mathbf{x}_2\Big] \quad (17)$$

Substituting the second constraint into Eq. (17) yields the required singular arc control law:

$$\boldsymbol{Q}_{\text{pto}}^{\text{sa}} = \bar{\boldsymbol{Q}}_{\text{ext}} + \bar{\boldsymbol{Q}}_{\text{rad}} - \boldsymbol{D}\mathbf{x}_2 - \bar{\boldsymbol{K}}\mathbf{x}_1 + \bar{\boldsymbol{M}}\Big(\bar{\boldsymbol{M}}^{-T}\frac{\partial \bar{\boldsymbol{Q}}_{\text{rad}}}{\partial \mathbf{x}_2} - \bar{\boldsymbol{C}}_2\Big)^{-1}\Big[\bar{\boldsymbol{M}}^{-1}\frac{\partial}{\partial x_3}\Big(\bar{\boldsymbol{Q}}_{\text{ext}} + \bar{\boldsymbol{Q}}_{\text{rad}}\Big) - \bar{\boldsymbol{C}}_3\frac{\partial \boldsymbol{Q}_{\text{pto}}}{\partial x_3} + \Big((\bar{\boldsymbol{M}}^{-T}\frac{\partial^2 \bar{\boldsymbol{Q}}_{\text{rad}}}{\partial \mathbf{x}_2 \partial x_3}) - \bar{\boldsymbol{C}}_1\Big)\mathbf{x}_2\Big] \quad (18)$$

From the necessary condition in Eq. (13) one can write:

$$\mathbf{x}_2 = \Big[\Big(\bar{\boldsymbol{M}}^{-T}\frac{\partial \boldsymbol{Q}_{\text{rad}}}{\partial \mathbf{x}_2}\Big) - \bar{\boldsymbol{C}}_2\Big]^{-1}\Big(\bar{\boldsymbol{C}}_1 \mathbf{x}_1 - \bar{\boldsymbol{M}}^{-1}(\boldsymbol{Q}_{\text{hydro}}) + \bar{\boldsymbol{C}}_3 \boldsymbol{Q}_{\text{pto}} - \boldsymbol{C}\Big) \quad (19)$$

The expression above can also be obtained by substituting the second constraint into Eq. (18) and then integrating. By integrating Eq. (19) one can get:

$$\mathbf{x}_1 = \int_{t_0}^{t}\Bigg(\Big[\Big(\bar{\boldsymbol{M}}^{-T}\frac{\partial \bar{\boldsymbol{Q}}_{\text{rad}}}{\partial \mathbf{x}_2}\Big) - \bar{\boldsymbol{C}}_2\Big]^{-1}\Big(\bar{\boldsymbol{C}}_1 \mathbf{x}_1 + \bar{\boldsymbol{C}}_3 \boldsymbol{Q}_{\text{pto}} - \bar{\boldsymbol{M}}^{-1}\Big(\bar{\boldsymbol{Q}}_{\text{ext}} + \boldsymbol{Q}_{\text{rad}}\Big) - \boldsymbol{C}\Big)\Bigg) d\sigma + \mathbf{x}_1(t_0) \quad (20)$$

Since t_0 is arbitrary, it can be proved that the constant $\boldsymbol{C} = \mathbf{0}$ by substituting $t = t_0$.

The derivatives of the generalized radiation force are required for the switching surface obtained by substituting $\boldsymbol{C} = \mathbf{0}$ in Eq. (15) and the singular arc generalized forces in Eq. (18). From Eq. (5), and the differentiation under the integral sign rules, one can write:

$$\frac{\partial \bar{\boldsymbol{Q}}_{\text{rad}}}{\partial x_3} = -\bar{\boldsymbol{K}}(0)\mathbf{x}_2(t) - \int_0^t \Big(\dot{\bar{\boldsymbol{K}}}(t-\tau)\mathbf{x}_2(\tau)\Big)\, d\tau \quad (21)$$

$$\frac{\partial \bar{\boldsymbol{Q}}_{\text{rad}}}{\partial \mathbf{x}_2} = -\int_0^t \Big(\bar{\boldsymbol{K}}^T(t-\tau)\Big)\, d\tau \quad (22)$$

$$\frac{\partial^2 \bar{\boldsymbol{Q}}_{\text{rad}}}{\partial x_3 \partial \mathbf{x}_2} = -\bar{\boldsymbol{K}}^T(0) - \int_0^t \Big(\dot{\bar{\boldsymbol{K}}}^T(t-\tau)\Big)\, d\tau \quad (23)$$

For regular waves, the generalized radiation force can be expressed as $\bar{\boldsymbol{Q}}_{\text{rad}}(x_3) = \bar{\boldsymbol{D}}_{\text{rad}}\mathbf{x}_2$ [6], using this expression, one can substitute into the first necessary condition expressed by Eq. (15) to obtain the switching condition:

$$\dot{H}_u = \bar{\boldsymbol{C}}_3 \boldsymbol{Q}_{\text{pto}} + \bar{\boldsymbol{C}}_2 \mathbf{x}_2 + \bar{\boldsymbol{C}}_1 \mathbf{x}_1 - \bar{\boldsymbol{M}}^{-1}\bar{\boldsymbol{Q}}_{\text{ext}} + \boldsymbol{C} = \mathbf{0} \quad (24)$$

where for regular waves $\bar{\boldsymbol{C}}_2 = (\bar{\boldsymbol{M}}^{-1}\bar{\boldsymbol{D}} + (\bar{\boldsymbol{D}}\bar{\boldsymbol{M}}^{-1})^T)$, and $\bar{\boldsymbol{D}} = \boldsymbol{D} + \bar{\boldsymbol{D}}_{\text{rad}}$. Similarly, from Eq. (18) and the expression of generalized PTO force for regular waves becomes:

$$\boldsymbol{Q}_{\text{pto}}^{\text{sa}} = \bar{\boldsymbol{Q}}_{\text{ext}} - \bar{\boldsymbol{D}}\mathbf{x}_2 - \bar{\boldsymbol{K}}\mathbf{x}_1 - \bar{\boldsymbol{M}}\bar{\boldsymbol{C}}_2^{-1} \times \left[\bar{\boldsymbol{M}}^{-1}\frac{\partial \bar{\boldsymbol{Q}}_{\text{ext}}}{\partial x_3} - \bar{\boldsymbol{C}}_1\mathbf{x}_2 - \bar{\boldsymbol{C}}_3\frac{\partial \boldsymbol{Q}_{\text{pto}}}{\partial x_3}\right] \quad (25)$$

Definition 1. *For VSB WECs, a control law that maintains*

$$H_u(\mathbf{x}, \boldsymbol{\lambda}) = 0, \quad \forall t \in [t_1, t_2] \subseteq [t_0, t_f] \quad (26)$$

for the optimal control problem defined in section II-B, if a singular control exists, the problem becomes a singular optimal control problem. The optimal control law thus consists of subarcs of singular control, and non-singular (bang) control, and it is determined by the sign of the switching curves defined by the components of "$\boldsymbol{C}$", and the junctions between the control laws are discontinuous. We say a singular arc occurs if any of the switching functions $C_i \forall i = 1, ..., N_p$ vanishes; C_i is defined as the switching surface that corresponds to Q_i^{pto} and it is obtained from the necessary condition $\dot{H}_{u_i}$. The optimal control law that satisfies the two additional necessary conditions $\dot{H}_u$, $\ddot{H}_u$ and Legendre-Clebsch Condition $:= (-1)^k \frac{d}{du}\left(\frac{d^{2k}}{dx_3^{2k}}\right) H_u \geq 0$ $\forall t \in [t_1 \;\; t_2]$ *is expressed as* $\boldsymbol{Q}^{pto} = \begin{cases} \boldsymbol{Q}_{pto}^{sa} & \text{if } \boldsymbol{C} = \mathbf{0} \\ \boldsymbol{Q}_{pto}^{max} & \text{if } \boldsymbol{C} < \mathbf{0} \\ \boldsymbol{Q}_{pto}^{min} & \text{if } \boldsymbol{C} > \mathbf{0} \end{cases}$. *The optimal* $\boldsymbol{Q}_{pto}$ *components switch from one boundary to the other at the zero crossings of the corresponding function.*

IV. MAIN RESULTS

In this section, the optimal control solutions of spherical VSB and FSB WECs in regular and irregular waves, are presented. For the VSB, two models are tested: (1) No control on the buoy shape, and (2) Optimally controlled shape using distributed piezoelectric actuators/harvesters. The deformation is controlled actively depending on the wave conditions; the shape motion is described by the mode shapes. The derived control laws determine the amplitudes of the mode shapes that give the optimal buoy shape. The outer diameter and the shell thickness of the buoys are 2.5 m and 0.3 m. The modulus of Elasticity of the FSB is 10 GPa compared to 1 MPa for the VSB, the material Poisson's ratio is $\nu = 0.3$, and $N = 3$. In this section, the VSB WEC SC denotes the shape-controlled VSB WEC.

Assumption 1. *Love's approximation is applied to derive the shell dynamics, i.e., thin shell, and small shell deformations are assumed.*

Assumption 2. *The steady-state vibration response of the shell is axisymmetric. i.e., no out-of-plane vibrations.*

Assumption 3. *The PTO unit, and the shape actuators/harvesters' dynamics are ignored.*

For the regular wave, the wave height and period are 0.8222 m and 6 sec, respectively. The simulation was done over a period of 1000 seconds with PTO saturation limits of $\boldsymbol{Q}_{\text{pto}}^{\max} = -\boldsymbol{Q}_{\text{pto}}^{\min} = \begin{bmatrix}6 & 1 & 1 & 1\end{bmatrix}^T \times 10^4$ N. The pk-pk displacement of both VSB WECs decreased by 3.5% compared to the FSB WEC; on the other hand, the pk-pk velocity increased by 2.7% compared to the FSB WEC.

There is an increase in the harvested energy for the VSB WEC and VSB WEC SC compared to the FSB WEC, as shown in Fig. 2. This suggests that for a VSB WEC and a FSB WEC to harvest similar energy, the VSB WEC will require much less reactive power, which makes it economically more appealing. The bidirectional power behavior can also be noticed as the energy curves are non-monotonic. The VSB WEC SC harvested 7% more energy compared to the VSB WEC. Also, the VSB WEC SC and the VSB WEC harvested 40.4% and 31% more energy compared to the theoretical limit (TL) of the FSB WEC as shown in Fig. 2. Furthermore, there is a decrease in the required reactive powers for both VSB WEC and VSB WEC SC of 8.77% and 10.73%, respectively, compared to the FSB WEC.

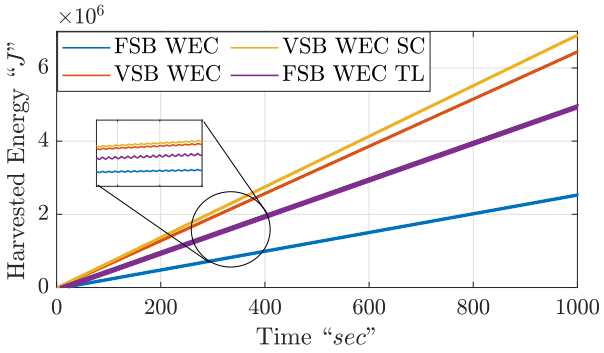

Fig. 2. Regular Wave: Harvested Energy

To model an irregular wave, a Bretschneider Spectrum is implemented with a significant wave height and peak wave period of 0.8222 m and 6 sec, respectively. The number of frequencies is $N_w = 256$. A simulation for 360 seconds is conducted using the same PTO force saturation limits as the regular wave case. Simulations show that the heave displacement of the VSB WEC SC is less than the FSB WEC and the VSB WEC; The root mean square value (RMS) of heave displacement for the FSB, VSB WEC, and VSB WEC SC are 0.39, 0.37, and 0.34 m, respectively. The RMS of their velocities are 0.58, 0.52, and 0.49 m/sec, respectively.

The harvested energy from the VSB WEC and the VSB WEC SC increased over that of the FSB WEC by 11.04% and 26.93%, respectively. Also, the VSB WEC harvests almost the same amount of energy as the theoretical limit of the FSB WEC.It is important to highlight that the harvested energies of the VSB WECs are higher than that of the FSB WEC even though the RMS velocities are less; this is due to the continuously changing shape of the buoy. Being able to capture more power with about the same heave motion is indeed a new phenomenon in wave energy conversion. This can be further justified using Fig. 4 in which the VSB WECs SC require less negative power compared to FSB WEC, where there is a reduction in the reactive powers for the VSB WEC and the VSB WEC SC of 11.9% and 17.4%, respectively, compared to the FSB WEC.

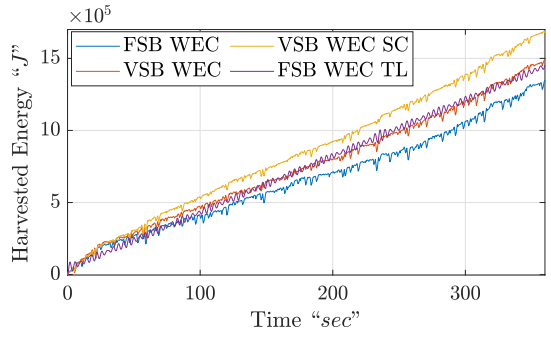

Fig. 3. Irregular wave: Harvested Energy

To provide an insight into the efficiency of VSB WECs compared to the FSB WEC, the capture width ratio (CWR) for the three devices was calculated based on Ref. [20], the CWR for irregular waves is defined as the ratio between the mean absorbed power "$p_m(W)$" by the WEC to the wave energy transport "$p_w = \frac{1}{2}\rho g \int_{\omega_{\min}}^{\omega_{\max}} \frac{S(\omega)}{\omega} d\omega (W/m)$" multiplied by the characteristic dimension of the buoy "$D(m)$", i.e., $CWR = \frac{p_m}{Dp_w}$, where $S(\omega)$ is the wave spectrum at frequency ω. The CWR of the FSB WEC, VSB WEC, and VSB WEC SC are 0.15, 0.19, and 0.21, respectively.

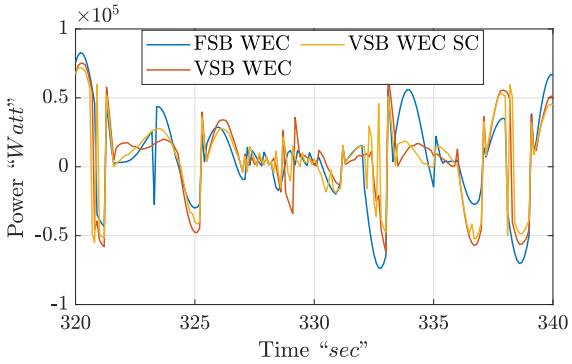

Fig. 4. Irregular wave: PTO Power

V. CONCLUSIONS AND FUTURE WORK

The optimal control laws for the *variable-shape wave energy converters* were derived using Pontryagin's minimum principle, and the control laws for the C.G. and the buoy shape are found to have a bang-singular-bang behavior. The VSB WEC, with and without shape control, requires less reactive power while harvesting more amount of energy compared to the FSB WEC, which makes it economically more appealing. For future work, the dynamics of the PTO force and the smart material harvesters/actuators should be included in the dynamic equation, and the positive power bang-singular-bang control law (PPBSB) should be tested to assess the amount of reactive power needed for the tested WECs.

ACKNOWLEDGMENT

This material is supported by the National Science Foundation (NSF), USA, under grant number 2023436. The research reported in this paper is partially supported by the HPC@ISU equipment at Iowa State University, some of which has been purchased through funding provided by NSF under MRI grant number 1726447.

REFERENCES

[1] A. Clément, P. McCullen, A. Falcão, A. Fiorentino, F. Gardner, K. Hammarlund, G. Lemonis, T. Lewis, K. Nielsen, S. Petroncini, *et al.*, "Wave energy in europe: current status and perspectives," *Renewable and sustainable energy reviews*, vol. 6, no. 5, pp. 405–431, 2002.

[2] A. Pecher and J. P. Kofoed, *Handbook of ocean wave energy*. Springer Nature, 2017.

[3] A. A. Hamada and M. Furth, "Numerical simulation of the effect of buoy geometries on pto of wave energy converters," in *SNAME Maritime Convention*, OnePetro, 2021.

[4] A. A. Hamada, A. Rolen, W. McCullough, and M. Furth, "Numerical simulation of the effect of wave characteristics on pto of point absorber wave energy converter," in *SNAME 27th Offshore Symposium*, OnePetro, 2022.

[5] W. Cummins, "The impulse response function and ship motions," 1962.

[6] M. A. Shabara and O. Abdelkhalik, "Dynamic modeling of the motions of variable-shape wave energy converters," *Renewable and Sustainable Energy Reviews*, vol. 173, p. 113070, 2023.

[7] M. A. Shabara and O. Abdelkhalik, "On the dynamics of variable-shape wave energy converters," 2022.

[8] J. Song, O. Abdelkhalik, R. Robinett, G. Bacelli, D. Wilson, and U. Korde, "Multi-resonant feedback control of heave wave energy converters," *Ocean Engineering*, vol. 127, pp. 269–278, 2016.

[9] D. García-Violini, Y. Peña-Sanchez, N. Faedo, and J. V. Ringwood, "An energy-maximising linear time invariant controller (lite-con) for wave energy devices," *IEEE Transactions on Sustainable Energy*, vol. 11, no. 4, pp. 2713–2721, 2020.

[10] S. Zou, O. Abdelkhalik, R. Robinett, G. Bacelli, and D. Wilson, "Optimal control of wave energy converters," *Renewable energy*, vol. 103, pp. 217–225, 2017.

[11] G. Bacelli, *Optimal control of wave energy converters*. National University of Ireland, Maynooth (Ireland), 2014.

[12] G. Nolan, J. Ringwood, S. Butler, and W. Leithead, "Optimal damping profiles for a heaving buoy wave energy converter," in *The fifteenth international Offshore and Polar Engineering conference*, OnePetro, 2005.

[13] M. P. Schoen, J. Hals, and T. Moan, "Wave prediction and fuzzy logic control of wave energy converters in irregular waves," in *2008 16th Mediterranean conference on control and automation*, pp. 767–772, IEEE, 2008.

[14] E. Anderlini, D. I. Forehand, P. Stansell, Q. Xiao, and M. Abusara, "Control of a point absorber using reinforcement learning," *IEEE Transactions on Sustainable Energy*, vol. 7, no. 4, pp. 1681–1690, 2016.

[15] S. Zou, X. Zhou, I. Khan, W. W. Weaver, and S. Rahman, "Optimization of the electricity generation of a wave energy converter using deep reinforcement learning," *Ocean Engineering*, vol. 244, p. 110363, 2022.

[16] E. Abraham and E. C. Kerrigan, "Optimal active control and optimization of a wave energy converter," *IEEE Transactions on Sustainable Energy*, vol. 4, no. 2, pp. 324–332, 2012.

[17] J. Falnes and A. Kurniawan, *Ocean waves and oscillating systems: linear interactions including wave-energy extraction*, vol. 8. Cambridge university press, 2020.

[18] M. A. Shabara, S. Zou, and O. Abdelkhalik, "Numerical investigation of a variable-shape buoy wave energy converter," in *International Conference on Offshore Mechanics and Arctic Engineering*, vol. 85192, p. V009T09A013, American Society of Mechanical Engineers, 2021.

[19] M. A. Shabara and O. Abdelkhalik, "Bang-bang control of spherical variable-shape buoy wave energy converters," in *2022 American Control Conference (ACC)*, pp. 3094–3099, 2022.

[20] O. Abdelkhalik, S. Zou, R. D. Robinett, G. Bacelli, D. G. Wilson, R. Coe, and U. Korde, "Multiresonant feedback control of a three-degree-of-freedom wave energy converter," *IEEE Transactions on Sustainable Energy*, vol. 8, no. 4, pp. 1518–1527, 2017.